

# PROCEEDINGS OF SPIE

[SPIDigitalLibrary.org/conference-proceedings-of-spie](https://spiedigitallibrary.org/conference-proceedings-of-spie)

## Properties of Yb doped silica fibers with different Al and P co-dopants concentrations produced by the Sol-Gel based granulated silica method

Ali El Sayed, Soenke Pilz, Jonas Scheuner, Hossein Najafi, Thomas Feurer, Valerio Romano

Ali El Sayed, Soenke Pilz, Jonas Scheuner, Hossein Najafi, Thomas Feurer, Valerio Romano, "Properties of Yb doped silica fibers with different Al and P co-dopants concentrations produced by the Sol-Gel based granulated silica method," Proc. SPIE 10681, Micro-Structured and Specialty Optical Fibres V, 1068105 (9 May 2018); doi: 10.1117/12.2323493

**SPIE.**

Event: SPIE Photonics Europe, 2018, Strasbourg, France

source: <https://doi.org/10.24451/arbor.7538> | downloaded: 5.12.2022

# Properties of Yb doped silica fibers with different Al and P co-dopants concentrations produced by the Sol-Gel based granulated silica method

Ali El Sayed<sup>\*a,b</sup>, Soenke Pilz<sup>b</sup>, Jonas Scheuner<sup>a</sup>, Hossein Najafi<sup>b</sup>, Thomas Feurer<sup>a</sup>, Valerio Romano<sup>a,b</sup>

<sup>a</sup>Institute of Applied Physics, University of Bern, Sidlerstrasse 5, Bern 3012, Switzerland;

<sup>b</sup>ALPS, Bern University of Applied Sciences, Pestalozzistrasse 20, Burgdorf 3400, Switzerland

## ABSTRACT

The sol-gel based granulated silica method has several advantages for the production of active optical fibers. It offers a high degree of freedom regarding the usable dopants and co-dopants, the maximum possible dopant concentration and the homogeneity of the dopants. The freedom in controlling the co-dopant concentration enables the full control to tailor the refractive index of the core. Several ytterbium (Yb) doped, aluminum (Al) and phosphorus (P) co-doped double cladding silica fibers with varying Al and P co-dopants concentrations have been produced by the sol-gel based granulated silica method, in order to study the influence of the different co-dopants concentrations on the fibers performance. To do so, we fixed the Yb concentration to 0.3 at% in all the fibers, as well as the cores and claddings diameters to 10 and 125 micrometer respectively. The variation of the core-cladding refractive index steps due to the different Al and P co-dopants concentration have been confirmed by measuring the one dimensional and two dimensional refractive index profile of every fiber by two different measurement apparatus, resulting in core-cladding refractive index steps that correspond well with the fibers compositions. In addition, the effect of the different co-dopants concentration on the fibers performance have been investigated by measuring the upper state lifetimes and the lasing performance (slope efficiency) of the fibers. We observed different fluorescence lifetimes among the differently co-doped fibers, and different slope efficiencies that are well correlated with the corresponding lifetime of each fiber. One of the fibers featured 60% slope efficiency at 1030nm by pumping the fiber at 976nm by a fiber-pigtailed laser diode (LD).

**Keywords:** Solgel, granulated silica, ytterbium doped fibers, lifetime, slope efficiency

## 1. INTRODUCTION

Over the last few years, rare earth (RE) doped silica glass fibers have attracted increasing interest for the development of fiber amplifiers and fiber lasers[1]–[5]. Ytterbium doped silica fibers are of particular interest due to their numerous advantages, such as simple energy level diagram with only two electronic multiplets (2F5/2 and 2F7/2), long fluorescence lifetime, broad absorption and emission bands and high quantum efficiency[6]–[8]. All these features make ytterbium doped silica fibers exceedingly implemented in optical amplifiers and fiber lasers, and especially in high power laser systems for applications requiring bright and high power beam, such as material processing, medicine and telecommunication[9]–[11]

Most rare-earth-doped silica glass fiber preforms are well known to be fabricated using the traditional modified chemical vapor deposition (MCVD) method because of its excellent degree of achievable purity and low optical loss[12], [13]. However, MCVD has its geometrical limitation, it's mainly suited for fiber shapes with a cylindrical symmetry with restriction in the core size by the reason of homogeneity. Furthermore, with MCVD it is difficult to maintain proper control over the preform/fiber parameters such as the dopant concentration, the usable dopants, the compositional homogeneity, and the dopant distribution[10], [14].

With our sol-gel-based granulated silica method we overcome some of the fabrication constraints of the conventional techniques by combining the benefits of the sol-gel based granulate/powder with the advantages of the powder-in-tube

technique. In comparison with the conventional techniques, one of the advantages offered by the sol-gel method is that doped silica material of high purity can be obtained at temperature below 2000 C[15]-[16]. Furthermore, combining the sol-gel method with the granulated silica method offers on one hand high degree of freedom concerning the dopants and co-dopants composition and their concentration, and on the other hand more control over the fiber geometry and microstructure[17]–[19]. This freedom in controlling the co-dopants and their concentration enables a very high level of control over the refractive index of the core, which results in optical fibers with the desired refractive index contrast. Using the sol-gel based granulated silica method, several Yb doped, Al and P co-doped double cladding silica fibers with a fixed Yb dopant concentration of 0.3at% and varying aluminum and phosphorus co-dopants concentrations have been produced. Core-cladding refractive index steps that varies between 0.0025 and 0.01 have been measured using two different refractive index profilers. In this paper, we describe the production method of the realized fibers, the measurements of their refractive index profiles, and the effect of the Al and P co-dopants concentration on the fibers performance by investigating their fluorescence lifetime and lasing performance.

## 2. FIBRE PRODUCTION BY THE SOL-GEL GRANULATED SILICA METHOD

### 2.1. Method Description

The basic principle and development of the granulated silica method based on the sol-gel process for active fiber production has been previously described in details in [20]–[22].

Taking place at room temperature, the sol-gel process starts with mixing silica and dopants precursors (metal alkoxides and water soluble RE, aluminum and phosphorus compounds) in the liquid phase, see Figure 1&2. Since the process starts in the liquid phase, the dopants precursors are homogeneously dissolved, allowing high dopant concentrations (up to several at.%) [19]. Additionally, the simplicity and flexibility of the sol-gel process enables a greater freedom in adaptable dopants. Furthermore it has been reported that silica powder based on the sol-gel method can show lower impurities compared with natural quartz powder which is commonly used for pure silica glass [23]. Therefore the sol-gel method is very well suited to make doped material for the production of rare earth doped fibers.

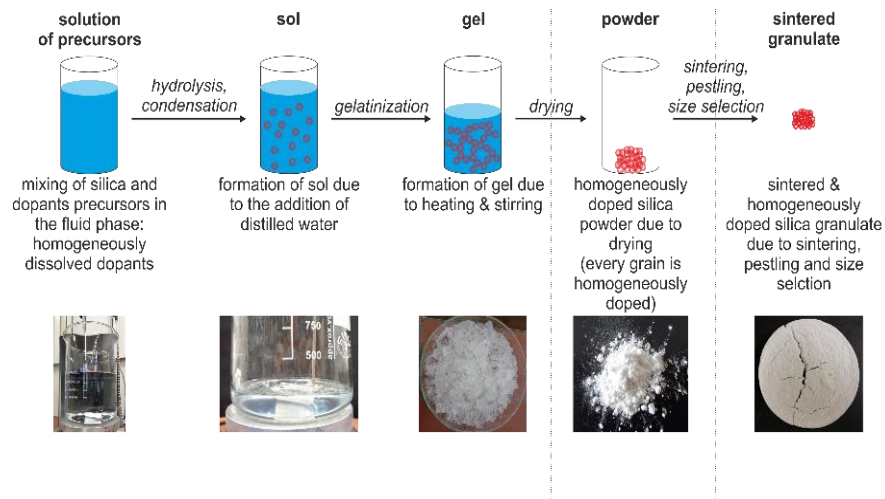


Figure 1. Basic principle of our developed and refined sol-gel process approach [22]

By the addition of distilled water and heating, the solution of precursors undergoes hydrolysis, condensation, gelatinization and drying, resulting finally in a powder [21], [22]. The dried powder resulting from the sol-gel process is then sintered, ground and sieved, yielding coarse granulated silica with a grain size of several 100 μm where every grain is homogeneously doped [22].

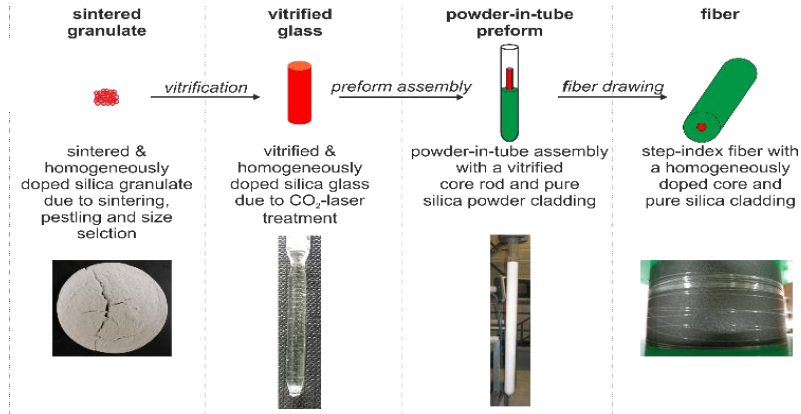


Figure 2. Overview of the vitrification of the sintered powder, preform assembling and fiber drawing [22].

After obtaining the doped granulated silica by sol-gel, the doped powder can be directly used for powder-in-tube preform assembly. However, we found that this leads to large scattering losses in the order of 1 dB/m due to micro-bubble formation and the absorption of water and impurities. Significant improvements in the fiber propagation and reduction in the scattering losses in the resulting fiber can be achieved by adding an intermediate vitrification step before fiber drawing, e.g. using CO<sub>2</sub> laser based small zone vitrification [20]-[21].

## 2.2. Fabrication of Yb Doped, Al and P Co-doped Silica Fibers by the Sol-Gel Granulated Silica Method

Due to all of the special characteristics mentioned in the introduction and since we are interested in fabricating a fiber with emission within the near infrared region of 1000-1100nm, the rare earth (RE) element ytterbium (Yb) is our active element of choice. It is well known that the properties of silica based Yb doped fibers can be influenced and improved by combining further co-dopants. For this purpose, we used two optically passive co-dopants: aluminum (Al) and phosphorous (P). Aluminum is used, since it is known to increase the solubility and prevent clustering of Yb atoms [24]-[25]. While by adding phosphorous (P), the photodarkening loss is strongly reduced [26], [25].

However, the optimum concentrations of the aluminum and phosphorus co-dopants with respect to each other it is still not clear. Therefore, to study the effects of the different co-dopants concentration, four fibers with a fixed ytterbium concentration (of 0.3 at.%) and varying aluminum and phosphorus concentrations have been prepared with the sol-gel based granulated silica method.

For the sol-gel process, we used tetraethyl orthosilicate (TEOS: Si(OC<sub>2</sub>H<sub>5</sub>)<sub>4</sub>) as silica precursor, ytterbium(III) nitrate pentahydrate (Yb(NO<sub>3</sub>)<sub>3</sub>·5H<sub>2</sub>O) as ytterbium dopant precursor, and as optically passive co-dopant the precursors aluminum nitrate nonahydrate (Al(NO<sub>3</sub>)<sub>3</sub>·9H<sub>2</sub>O) and phosphorus pentoxide (P<sub>2</sub>O<sub>5</sub>). The core precursor compositions for the produced fibers are listed in Table 1.

Table 1. Core precursor composition

	F1	F2	F3	F4
Yb / at. %	0.3	0.3	0.3	0.3
Al/P / at. %	4.8	2	1	0.8

After obtaining the doped granulated silica from the sol-gel process, the doped powder was vitrified into rod preform. The vitrification is based on a CO<sub>2</sub> laser treatment at 100W and on small zone vitrification technique. The vitrification process was realized in collaboration with APRI (Advanced Photonics Research Institute: Gwangju Institute of Science and technology, South Korea) and Taihan Fiberoptics (TFO: South Korea). The complete fiber preform is then obtained by placing the vitrified core rod in the center of a large silica tube. At about 2000C the assembled preform was drawn into a fiber with a core of 10 microns of diameter and a cladding of 125 microns of diameter. Finally, the fiber was coated with low index coating in order to obtain a double-clad Yb doped fiber.

### 3. MEASUREMENTS AND RESULTS

#### 3.1. Refractive Index Profiles

The refractive index profile is one of the essential parameters to determine various properties of optical fiber such as, the numerical aperture and the single mode cutoff. Bubnov [27], studied the effect of aluminum and phosphorus concentrations on the refractive index in silica glass. Showing that both co-dopants by their own would individually increase the refractive index, but in combination, the phosphorous compensates the refractive index change arising from the aluminum [28].

To confirm the effect of the aluminum and phosphorus concentration on the refractive index steps, an accurate measurement of the refractive index profile is required. Therefore, the refractive index profile was measured by two different methods. The first one is a self-built inverse refracted near field technique, which is based on the refracted near field technique but modified in such a way that allows a 2-D measurement of the refractive index profile[29]–[31]. The second setup is a self-built reflection-based refractive index mapping setup with high measurement accuracy [32].

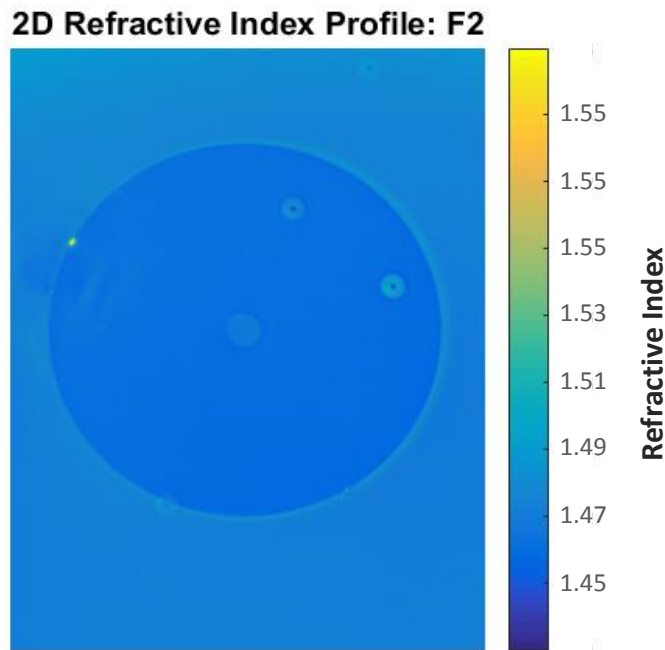


Figure 3. Two dimensional refractive index profile of F2 fiber, measured by the IRNF setup.

The measured refractive index step are summarized in table 2. The measured refractive index step correspond well with the Aluminum (Al) and phosphorus (P) co-dopant concentration in the fiber. The smaller the concentration ratio of Al/P

the smaller the refractive index contrast to the pure silica cladding and thus the smaller numerical aperture (NA). The two and one dimensional refractive index profile of fiber F1 are shown in Fig. 3&4

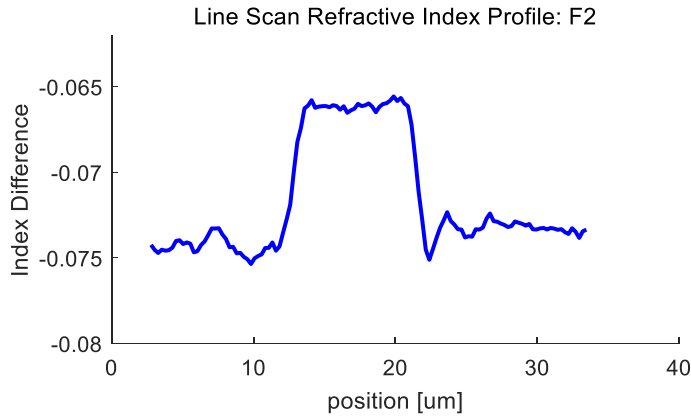


Figure 4. Refractive index profile of a one line scan over the cross section of fiber F2.

Table 2. Core precursor composition

	Fiber 1	Fiber 2	Fiber 3	Fiber 4
$\Delta n$	0.0095	0.0077	0.003	0.0027

### 3.2. Upper level excited state lifetime and lasing performance

One of the most important feature of Yb is the long upper level excited state lifetime (in the order of 1ms) that allows the storage of large energies in the excited state. Several unwanted mechanism such as multi-phonon decay and energy transfer between Yb ions, can result in quenching in the overall intensity of the fluorescence. Furthermore, the quenching process can be apparent as a reduction in the decay time of the excited Yb atoms. Therefore, the measurement of the excited state lifetime is of highly importance, as it indicates whether there are existing quenching, which could consequently influence the lasing performance of an Yb doped fiber.

To measure the fluorescence lifetimes of the 976nm emission of Yb, short fiber pieces were excited with a pulsed diode laser (915nm, 500mW) with rectangular pulses of 100 ms and a trailing edge slope of less than 5  $\mu s$ . The pump light was filtered away by using several long pass filters centered at 950nm and the generated and transmitted fluorescence emission at 975nm was detected using a photomultiplier with big sensitive area. Fluorescence decay curves were measured and evaluated. The decay curves were well described by a single exponential fit. The life time results vary between 0.75 and 0.9 ms and they are summarized in table 3. In addition, the fluorescence lifetime of a commercial Yb doped fiber [33] (Nufern: LMA-YDF-25/250-VIII) (Nufern, East Granby, Connecticut, USA) was measured for comparison.

Table 3. Fluorescence lifetime

	Fiber 1	Fiber 2	Fiber 3	Fiber 4	Commercial Fiber [33]
Lifetime [ms]	0.76	0.77	0.8	0.87	0.91

### 3.3. Laser characteristics

The laser characteristics of the Yb-doped Al and P co-doped silica fibers were tested. The fibers feature numerical apertures of the cores that vary between 0.08 and 0.15. The fibers were coated with low index coating resulting in double

cladding fibers with an inner-cladding numerical aperture of 0.48. For pumping the YDF, we consider the uses of cladding-pumping, which relaxes the requirements on pump beam quality and launch alignment. Another reason for the use of cladding-pumping is to allow a much higher incident pump power than could be tolerated, for damage reasons. For the cladding-pumping configuration, the absorption per unit length of pump light travelling in the inner cladding, without further measures, is therefore reduced by a factor approaching the ratio of the areas of the inner cladding and the core, compared to direct core-pumping. However, this reduced absorption per unit length, can be simply compensated by using a combination of longer fiber length and a pump wavelength where there is strong pump absorption. In Yb doped silica fiber, the highest peak absorption occurs at 976 nm.

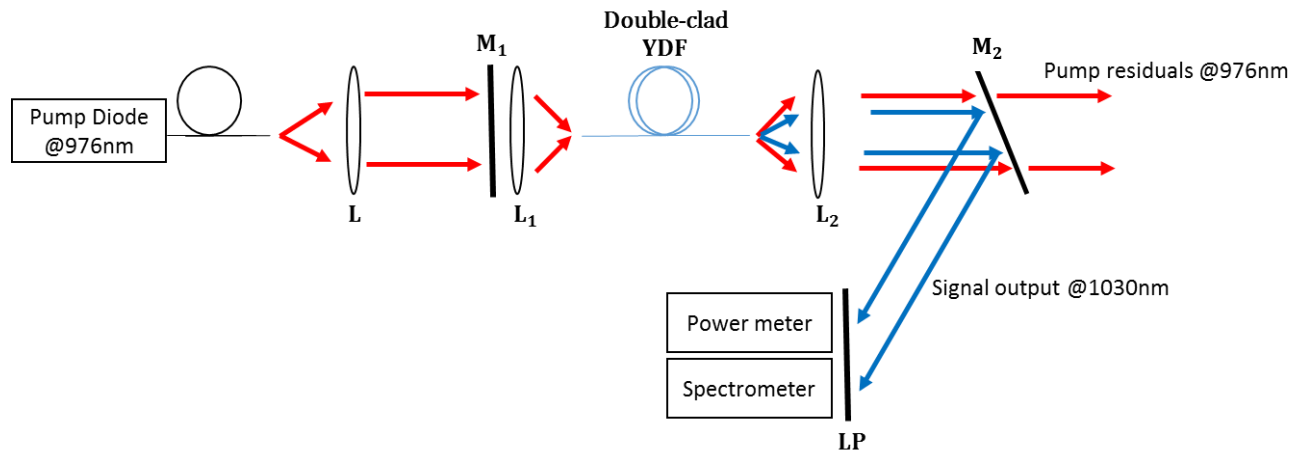


Figure 5. Yb-doped fiber laser arrangement, with fiber pigtailed pump diode source, lenses of 20mm focal length (L), in-coupling mirror ( $M_1$ ), dichroic mirror ( $M_2$ ), and a long pass filter centered at 1000nm (LP)

The experimental setup is shown in Figure 5. We used a forward pumping scheme with a fiber pigtailed laser diode (LD) with a silica fiber (NA 0.22) operating at 976nm with output power up to 20W. The pump beam was coupled into the double-clad Yb doped fiber using collimating and a focusing lenses, through a dichroic mirror ( $M_1$ ) with high transmission (HT) at 976nm and high reflection (HR) at 1030nm. On the output arm of the laser cavity, a feedback was provided the Fresnel reflection from the cleaved fiber end.

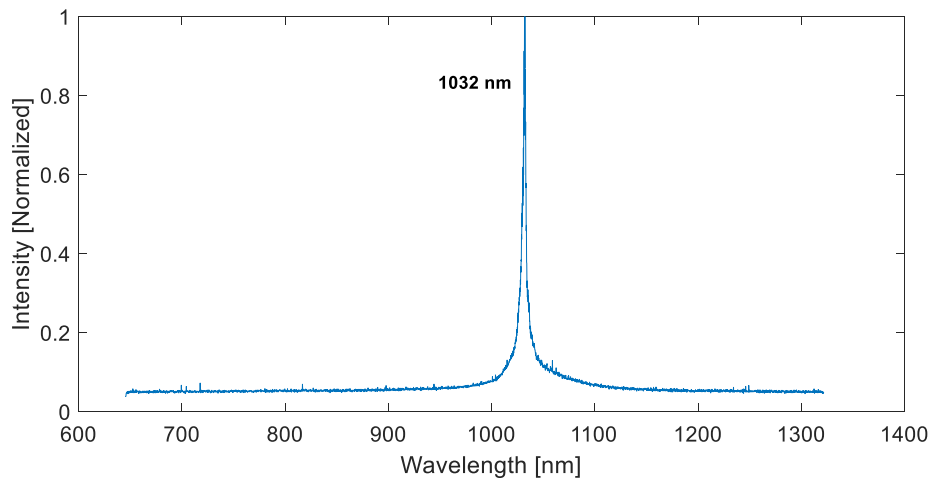


Figure 6. Laser output spectrum with an emission peak at around 1030nm.

The output signal from the YDF was separated from the pump beam using another dichroic mirror ( $M_2$ ). An additional long pass filters (LP) centered at 1000nm were used to make sure that no residual pump wavelength is in the signal beam. Finally, the spectrum of the laser output signal was measured by an Ocean Optics USB4000 spectrometer (Ocean Optics, Dunedin, FL, USA), Fig 6.

In order to compare the laser performance of the differently co-doped fibers, a fixed length of 3m of each fiber was tested, including the before mentioned mirror with high transmission (HT) at 976nm and high reflection (HR) at 1030nm on one side and a feedback provided by the 5% Fresnel reflection from the cleaved fiber end at the other side. Poor slope efficiencies at 1030nm were obtained for F1, F2 and F3 fibers, while 60% of slope efficiency was obtained for fiber F4 with threshold pump power of 700mW. The laser output power with respect to the absorbed pump power of fiber F4 is shown in Figure 7

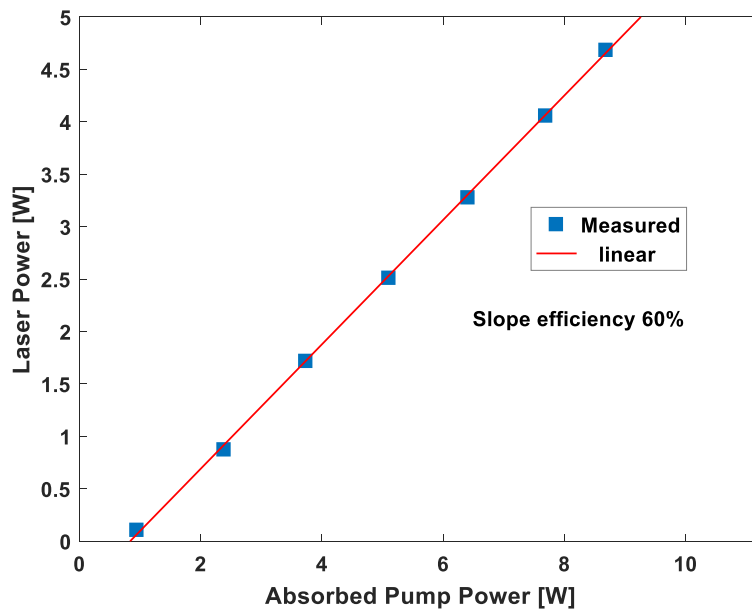


Figure 7. Laser output power at 1030nm versus absorbed pump power at 976nm of fiber F4.

#### 4. DISCUSSION AND CONCLUSION

The results show similar behavior of the pump absorption for the different fibers, with around 66% of absorbed pump power at 976nm in 3m of length, resulting in absorption coefficient of 1.6 dB/m. Considering the Yb concentration in the fibers and the overlap factor between the pumped and doped area (cladding pumped), the absorption cross section was estimated to be around  $1.5 \text{ } \mu\text{m}^2$ , which is in a good agreement with the absorption cross section of Yb doped aluminum phospho-silicate glasses found in literature [34]-[35]. The slope efficiencies were well correlated with the measured lifetimes of the Yb doped fibers. For F1, F2, and F3 fibers short lifetime decays were measured (around 0.75 ms), this indicates that there are some quenching mechanisms taking place in these fibers. Moreover, the quenching was also evident in the poor slope efficiencies of these fiber. There are many mechanisms which could take place and be responsible for the quenching of the overall intensity of the Yb fluorescence, among them Yb cluster formation leading to concentration quenching. This issue is still under investigation. On the other hand, fiber F4 with the highest phosphorus concentration showed the longest fluorescence lifetime decay (0.87ms). The lifetime is comparable with the value obtained for the Nufern LMA-YDF-25/250-VIII commercial fiber, this points towards no significant quenching taking place in the Yb atoms. The lasing performance of F4 fiber is well correlated with the measured fluorescence lifetime decay and confirms that there is no significant quenching, resulting in 60% of Slope efficiency for a fiber length of 3m pumped at 976nm. The laser total output power was around 5W and is limited by the available pump power. In summary, we have shown the



advantages of the sol-gel granulated silica method regarding the flexibility and simplicity of incorporating the dopant and co-dopants at room temperature, by fabricating several Yb-doped Al and P co-doped silica fibers. We have quantified the refractive index steps arising from different aluminum and phosphorus concentration, showing with that the high degree of flexibility offered by the production method regarding the precise control of the co-dopant concentrations which are maintained throughout the fabrication process. Finally, the effect of the fibers compositions on the lifetime and laser performance of the fibers was investigated, resulting in a superior performance of the fiber with the highest phosphorus concentration (lowest Al/P) compared to the other fibers.

## ACKNOWLEDGMENTS

We are very thankful to Ch. Bacher for active help in drawing the fibers and Y. Kim for discussions. Many thanks to David Kummer (BAUS), Stefan Berger, Andreas Ruefenacht, Martin Hochstrasser (Reseachem GmbH) and Georgios Karametaxas (SolSens GmbH) for their help in sol-gel material production and characterization. We also thank Woojin Shin from the APRI (Advanced Photonics Research Institute) in Gwangju Institute of Science and technology (Gwangju 500-712, South Korea) and TFO (Taihan Fiberoptics Co., LTD Gyeonggi-do / South Korea) for their efforts and contributions in the fiber vitrification and drawing processes. This work has been financially supported by the Swiss Commission for Technology and Innovation CTI under projects 7864.2 and 18613.

## REFERENCE

- [1] S. Ohara and Y. Kuroiwa, "Highly ytterbium-doped bismuth-oxide-based fiber," vol. 17, no. 16, pp. 14104–14108, 2009.
- [2] A. Dhar, M. C. Paul, M. Pal, A. K. Mondal, S. Sen, H. S. Maiti, and R. Sen, "Characterization of porous core layer for controlling rare earth incorporation in optical fiber," *Opt. Express*, vol. 14, no. 20, pp. 9006–9015, 2006.
- [3] A. Galvanauskas, "High Power Fiber Lasers," *Opt. Photonics News*, no. July, 2004.
- [4] J. Limpert, F. Roser, S. Klingebiel, T. Schreiber, C. Wirth, T. Peschel, R. Eberhardt, and A. Tiinnermann, "The Rising Power of Fiber Lasers and Amplifiers," *IEEE J. Sel. Top. Quantum Electron.*, vol. 13, no. 3, pp. 537–545, 2007.
- [5] Y. Li, J. Huang, Y. Li, H. Li, Y. He, S. Gu, G. Chen, L. Liu, and L. Xu, "Optical properties and laser output of heavily Yb-doped fiber prepared by Sol-Gel method and DC-RTA technique," *J. Light. Technol.*, vol. 26, no. 18, pp. 3256–3260, 2008.
- [6] M. R. a. Moghaddam, "Comparison between Analytical Solution and Experimental Setup of a Short Long Ytterbium Doped Fiber Laser," *Opt. Photonics J.*, vol. 02, no. 02, pp. 65–72, 2012.
- [7] S. Liu, H. Li, Y. Tang, and L. Hu, "Fabrication and spectroscopic properties of Yb 3 + -doped silica glasses using the sol-gel method," *Chinese Opt. Lett.*, vol. 10, no. 8, pp. 8–11, 2012.
- [8] W. Shikai, F. Suya, W. Meng, Y. Chunlei, Z. Qinling, L. Haiyuan, T. Yongxing, C. Danping, and H. Lili, "Optical and laser properties of Yb<sup>3+</sup>-doped Al<sub>2</sub>O<sub>3</sub>-P<sub>2</sub>O<sub>5</sub>-SiO<sub>2</sub> large-mode-area photonic crystal fiber prepared by the sol-gel method," *Laser Phys. Lett.*, vol. 10, no. 11, p. 115802, 2013.
- [9] Y. Jeong, J. Sahu, D. Payne, and J. Nilsson, "Ytterbium-doped large-core fiber laser with 1.36 kW continuous-wave output power.," *Opt. Express*, vol. 12, no. 25, pp. 6088–92, Dec. 2004.
- [10] S. Wang, F. Lou, M. Wang, C. Yu, S. Feng, Q. Zhou, D. Chen, and L. Hu, "Characteristics and Laser Performance of Yb<sup>3+</sup>-Doped Silica Large Mode Area Fibers Prepared by Sol-Gel Method," *Fibers*, vol. 1, no. 3, pp. 93–100, 2013.
- [11] W. L. Wentao Li, Q. Z. Qinling Zhou, L. Z. Lei Zhang, S. W. Shikai Wang, M. W. Meng Wang, C. Y. Chunlei Yu, S. F. Suya Feng, D. C. Danping Chen, and L. H. Lili Hu, "Watt-level Yb-doped silica glass fiber laser with a core made by sol-gel method," *Chinese Opt. Lett.*, vol. 11, no. 9, pp. 091601–91603, 2013.
- [12] S. R. Nagel, J. B. MacChesney, and K. L. Walker, "An Overview of the Modified Chemical Vapor Deposition (MCVD) Process and Performance," *IEEE Trans. Microw. Theory Tech.*, vol. 30, no. 4, pp. 305–322, 1982.
- [13] S. B. Poole, D. N. Payne, R. J. Mears, M. E. Fermann, and R. I. Laming, "Fabrication and Characterization of Low-Loss Optical Fibers Containing Rare-Earth Ions," *J. Light. Technol.*, vol. 4, no. 7, pp. 870–876, 1986.
- [14] J. J. Montiel i Ponsoda, L. Norin, C. Ye, M. Bosund, M. J. Söderlund, A. Tervonen, and S. Honkanen,

- “Ytterbium-doped fibers fabricated with atomic layer deposition method,” *Opt. Express*, vol. 20, no. 22, p. 25085, 2012.
- [15] D. . MacChesney, J.; Johnson, D.W., Jr.; Bhandarkar, S.; Bohrer, M.; Fleming, J.W.; Monberg, E.M.; Trevor, Ed., *In Sol-Gel Synthesis and Processing: Ceramic Transactions*. .
- [16] M. Locher, V. Romano, and H. P. Weber, “Rare-earth doped sol-gel materials for optical waveguides,” *Opt. Lasers Eng.*, vol. 43, no. 3–5, pp. 341–347, 2005.
- [17] U. Pedrazza, V. Romano, and W. Lüthy, “Yb<sup>3+</sup>:Al<sup>3+</sup>:sol-gel silica glass fiber laser,” *Opt. Mater. (Amst)*, vol. 29, no. 7, pp. 905–907, 2007.
- [18] R. Renner-Erny, L. Di Labio, and W. Lüthy, “A novel technique for active fibre production,” *Opt. Mater. (Amst)*, vol. 29, no. 8, pp. 919–922, 2007.
- [19] V. Romano, S. Pilz, and D. Etissa, “Sol-gel-based doped granulated silica for the rapid production of optical fibers,” *Int. J. Mod. Phys. B*, vol. 28, no. 12, p. 1442010, 2014.
- [20] J. Scheuner, A. M. Heidt, S. Pilz, P. Raisin, A. El Sayed, H. Najafi, M. Ryser, T. Feurer, and V. Romano, “Advances in optical fibers fabricated with granulated silica,” pp. 2–4.
- [21] S. Pilz, H. Najafi, A. El Sayed, J. Boas, D. Kummer, and J. Scheuner, “Progress in the fabrication of optical fibers by the sol-gel-based granulated silica method,” no. Mcvd.
- [22] S. Pilz, H. Najafi, M. Ryser, and V. Romano, “Granulated Silica Method for the Fiber Preform Production,” *Fibers*, vol. 5, no. 3, p. 24, 2017.
- [23] M. Tomozawa, D.-L. Kim, and V. Lou, “Preparation of high purity, low water content fused silica glass,” *J. Non. Cryst. Solids*, vol. 296, no. 1–2, pp. 102–106, 2001.
- [24] S. Unger, F. Lindner, C. Aichele, M. Leich, A. Schwuchow, J. Kobelke, J. Dellith, K. Schuster, and H. Bartelt, “A highly efficient Yb-doped silica laser fiber prepared by gas phase doping technology,” *Laser Phys.*, vol. 24, no. 3, 2014.
- [25] S. Unger, A. Schwuchow, S. Jetschke, V. Reichel, M. Leich, A. Scheffel, and J. Kirchhof, “Influence of aluminum-phosphorus codoping on optical properties of ytterbium-doped laser fibers,” vol. 7212, p. 72121B, 2009.
- [26] J. K. S. Unger, A. Schwuchow, S. Jetschke, V. Reichel, A. Scheffel, Ed., “Optical properties of Yb-doped laser fibers in dependence on codopants and preparation conditions.”
- [27] M. M. Bubnov, A. N. Gur’yanov, K. V. Zotov, L. D. Iskhakova, S. V. Lavrishchev, D. S. Lipatov, M. E. Likhachev, a a Rybaltovsky, V. F. Khopin, M. V. Yashkov, and E. M. Dianov, “Optical properties of fibres with aluminophosphosilicate glass cores,” *Quantum Electron.*, vol. 39, no. 9, pp. 857–862, 2009.
- [28] M. M. Bubnov, V. N. Vechkanov, A. N. Gur’yanov, K. V. Zotov, D. S. Lipatov, M. E. Likhachev, and M. V. Yashkov, “Fabrication and optical properties of fibers with an Al<sub>2</sub>O<sub>3</sub>-P<sub>2</sub>O<sub>5</sub>-SiO<sub>2</sub> glass core,” *Inorg. Mater.*, vol. 45, no. 4, pp. 444–449, 2009.
- [29] K. W. Raine, J. G. N. Baines, and D. E. Putland, “Refractive index profiling—state of the art,” *J. Light. Technol.*, vol. 7, no. 8, pp. 1162–1169, 1989.
- [30] M. Young, “Optical fiber index profiles by the refracted-ray method (refracted near-field scanning).,” *Appl. Opt.*, vol. 20, no. 19, pp. 3415–22, 1981.
- [31] A. El Sayed, S. Pilz, M. Ryser, and V. Romano, “Two-dimensional refractive index profiling of optical fibers by modified refractive near-field technique,” 2016, vol. 9744, no. , pp. 97440N–9744–8.
- [32] P. Raisin, J. Scheuner, V. Romano, and M. Ryser, “High-precision confocal reflection measurement for two dimensional refractive index mapping of optical fibers,” 2015, vol. 9507, no. , pp. 95070O–9507–6.
- [33] “[http://www.nuferm.com/pam/optical\\_fibers/907/LMA-YDF-25/250-VIII/](http://www.nuferm.com/pam/optical_fibers/907/LMA-YDF-25/250-VIII/).”
- [34] S. Jetschke, S. Unger, A. Schwuchow, M. Leich, and J. Kirchhof, “Efficient Yb laser fibers with low photodarkening by optimization of the core composition,” *Opt. Express*, vol. 16, no. 20, p. 15540, 2008.
- [35] M. A. Melkumov, I. A. Bufetov, M. M. Bubnov, K. S. Kravtsov, S. L. Semjonov, A. V. Shubin, and E. M. Dianov, “Ytterbium Lasers Based on P 2 O 5 - and Al 2 O 3 -doped Fibers,” no. 095, pp. 5–6, 2004.